ISSN: 2639-7455

Research Article

Earth & Environmental Science Research & Reviews

Light Penetration through Shallow Flowing Water, Comparing the Effects of Surface Lenses in Laminar Flow with Bubbles Added in Turbulent Flow

Swatland HJ

University of Guelph, Guelph, Ontario N1H 2Y8, Canada

*Corresponding author
Swatland HJ, University of Guelph, 33 Robinson Avenue, Guelph, Ontario N1H 2Y8, Canada

Submitted: 20 Feb 2020; **Accepted**: 29 Feb 2020; **Published**: 10 Mar 2020

Abstract

Penetration of light into water is important for aquatic photosynthesis. In shallow water, refraction at the water surface may result in bright and dark areas underwater, while turbulence increases both this surface lensing and shadowing by bubbles. Microscope measurements of static bubbles showed that, relative to their size, small bubbles cast stronger shadows than large bubbles. With moving water (depth ≈ 1 cm), optical fibers linked to photomultipliers showed turbulence changed the pattern of transmitted light, causing more, shorter and less intense peaks of light than in laminar flow. In laminar flow, light penetration was higher at 700 nm than at 470 nm. A wavelength difference was also found beyond the visible spectrum (850 > 365 nm).

Keywords: Laminar flow; Turbulent flow; Lensing; Shadowing; Light penetration; Photosynthesis

Introduction

Groundwater seeping from the Niagara Escarpment flows as small streams over step-like formations of rock strata and clay with flat sections separated by waterfalls [1]. This affects the pattern of CO_2 degassing which, in turn, is related to $CaCO_3$ deposition on surrounding mosses to form travertine [2]. In nearby rivers, similar step-like formations occur on a larger scale, with laminar flow on flat parts separated by turbulent flow in vertical parts. In stream ecology, flow dynamics and light for photosynthesis are both very important but the possible interactions between flow patterns and light penetration have received little or no attention [3]. Fluctuating light patterns are important for photosynthesis because a brief period to store the products of photosynthesis may allow optimum photon capture [4-6]. This effect is important for photosynthesis in mosses [7, 8].

The study starts with microscope spectrophotometry, measuring the effects of the refractive index boundary at the edges of static bubbles in water. The question was, how does bubble diameter affect shadowing? The dynamic aspects of underwater shadowing were studied using optical fibers to detect the flickering caused by surface lenses and bubbles. Blue light and red light are of particular interest for photosynthesis by chlorophyll b and chlorophyll a, respectively [9].

Two terms are used here in a special way. Lensing refers to refraction at a water surface. This is easily seen in an outdoor swimming pool with the sun as a point source illuminator. Waves on the water surface produce a reticular pattern on the bottom of the pool with bright lines around dull areas. The second term used here is shadowing, restricted to the shadows cast by reflective bubbles. From a distance, waterfalls appear white in daytime because the incident illumination is mostly reflected, thus it is dark under a waterfall because of shadowing. In nature, lensing and shadowing may overlap to a variable extent, as in the aquarium model used here. At a slow pump speed, there was a laminar flow with no bubbles over the sample chamber so that light fluctuations were caused by lensing. At a high pump speed, the water was turbulent with a highly variable surface and numerous bubbles. Thus, light fluctuations resulted from both lensing and shadowing.

It is important to explain how this study differs from a conventional approach to the attenuation of light in deep water [10]. In great depths of water, measured in many meters rather than a centimeter, blue light penetrates farther than red light, which is why deep divers find everything to be bluish. But in shallow freshwater streams over mosses, there may be only one or two centimeters of water – much less than what ecologists call shallow water [11]. Very shallow water effects might also occur on seashores at low tides, or have been important when plant life evolved from an aquatic to an aerial environment, not at great depths, but on shores with a shallow fluctuating water depth [12]. So this research is unusual in dealing with just the top centimeter of a shallow water column where surface lensing and shadowing dominate over deeper absorption following the Beer-Lambert law.

Experimental Methodology

Microscope Spectrophotometry

The microscope was a Zeiss Universal (Carl Zeiss, D-7082 Oberkochen, Germany) with accessories identified here by a Zeiss part number. The microscope was operated from a type MPC 64 control module (Zeiss 477469) on a bus (IEEE 488) [13]. The photomultiplier was a side-window Hamamatsu (1126 Ichino-Cho, Hamamatsu City, Japan) HTV R 928 with S-20 characteristics. A

grating monochromator (Zeiss 474345) with stray-light filters (Zeiss 477215) was mounted under the photomultiplier and scanned from 400 to 700 nm in steps of 10 nm with a 10 nm band-pass. Illumination was from a 100 W halogen source with a stabilized power supply (Hewlett-Packard 6642A) directed through a solenoid shutter. The photometer head was a type 03 (Zeiss 477304). Static bubbles were created in cavities on microscope slides using a pipette contaminated with detergent. Cover slips did not compress the bubbles.

Dynamic measurements

A bifurcated (Y-shaped) light guide was used to make dynamic measurements in water flowing in an aquarium (Figure 1). The common trunk of the light guide had an aperture 1mm in diameter with randomly arranged quartz optical fibers. The common trunk collected light which was then split into two branches leading through interference filters and to a matched pair of photomultipliers connected to high-speed analog to digital converters with buffers that could be unloaded to the computer when measuring was finished. The two photomultipliers (PmH-02, Sciencetech, London, Ontario) were adjusted to give the same output of 1 v before starting water flow. Wavelengths were controlled with interference filters mounted in filter wheels (Figure 1, B). The output voltage was read at 1 kHz using a Hewlett-Packard dual channel digitizer (E1429A in a VXI mainframe), which satisfied the Nyquist sampling rate requirement (the measuring rate must be faster than the frequency of the optical signal to avoid errors in a Moiré pattern). Illumination above the flowing water was from a tungsten filament (3 v, 0.9 a) located 15 cm above the light guide in the sample chamber. A stabilized DC power supply was used (HP 6642A). When static, the depth of water over the light guide was approximately 1 cm.

A key point was to cancel any possible differences in the response times of the two photomultipliers so inputs to photomultipliers were interchanged in a balanced pattern [14]. In other words, differences detected between wavelengths and between laminar and turbulent flow did not originate from a difference between the two photomultipliers

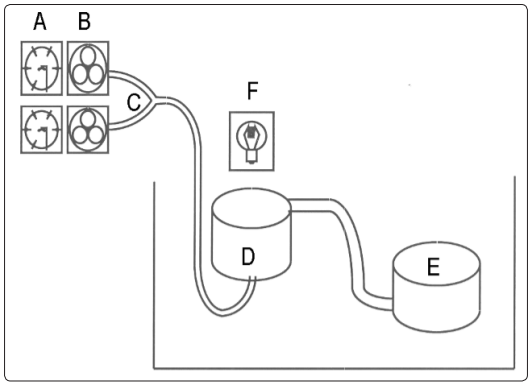

Figure 1: Apparatus for dynamic measurements in an aquarium. Two photomultipliers (A) with filter wheels to change wavelengths (B) were connected to a bifurcated light guide (C) with a common trunk in the base of a sample chamber (D). A pump (E) with flow rate controlled by a variable transformer produced a stream of water over the sample chamber. An illuminator (F) was located over the sample chamber.

To check on the apparatus, both recording channels were set to 700 nm and turbulent clear water was pumped over the common trunk of the light guide - both channels detected the same flicker pattern caused by bubbles (short duration) and lenses (long duration) on the turbulent water surface. These were counted and measured using an algorithm similar to one developed for signals from a fluorescence probe [15].

Results and Discussion

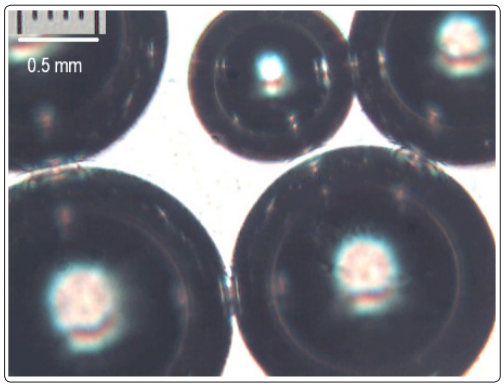

Figure 2: Becke lines around small bubbles.

The dark boundary around bubbles in transmitted light is the Becke line (Figure 2), named for Friedrich Becke (1855-1931). When a sample was lowered on the microscope stage so as to increase the distance between the sample and the objective lens of the microscope, the Becke line moved towards the higher refractive index [16]. With an air bubble in water, the Becke line moved toward the water. Consult Selmke for ray diagrams of light passing through bubbles [17].

When the microscope spectrophotometer was standardized on water to one side of an air bubble (transmittance, $T = 1$ at each wavelength), transmittance through the dark Becke line was very low ($T = 0.025 \pm 0.017$ at 400 nm to $T = 0.017 \pm 0.007$ at 700 nm). To understand the chromatic effects on light passing through a bubble, measurements were taken at the edge of a bubble, through the Becke line and through the axis of the bubble (Figure 3).

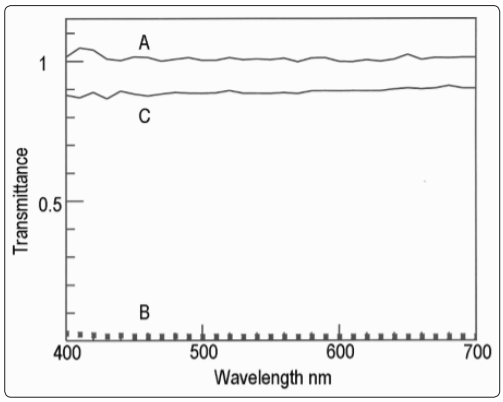

Figure 3: Transmittance through an 8-mm bubble, just outside the bubble (A), through the Becke line (B) and through the axis of the bubble (C)

For transmittance through the axes of bubbles (Figure 4), the source of the variance was the size of the bubble (from 0.5 to 8 mm), and the strongest correlation of transmittance with bubble diameter ($r = 0.88$, $P < 0.005$, $n = 9$) was at the low point of transmittance. This

was because, in small bubbles, the Becke line intruded on the optical axis of the bubble. Thus, relative to their size, small bubbles had a much stronger shadowing effect than large bubbles.

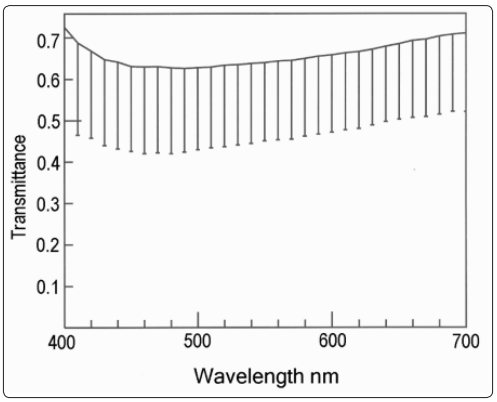

Figure 4: Transmittance through the optical axis of bubbles (mean value, n = 9, with error bars showing standard deviations caused by bubble diameter)

Dynamic measurements

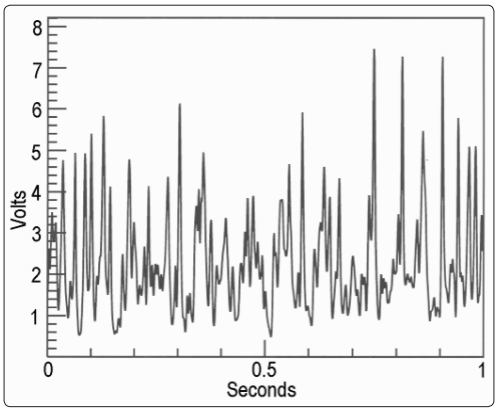

Figure 5: A laminar flow pattern

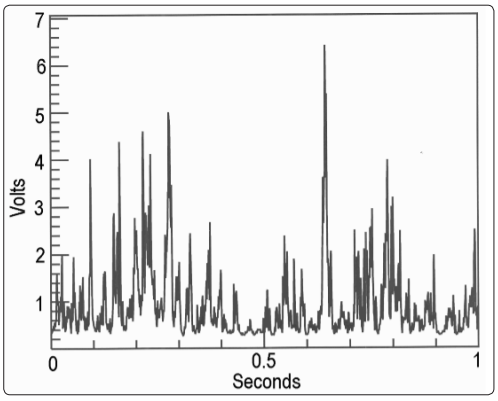

Figure 6: A turbulent flow pattern

Examples of laminar and turbulent flow patterns are show in Figures 5 and 6. No meaningful differences between wavelengths (470 vs 700 nm) were detected for peaks sec -1, mean peak v or mean peak width (Table 1). However, when these three parameters were multiplied together to estimate total light, more light at 700 nm than at 470 nm was transmitted through water in the sample chamber ($P < 0.01$) when the flow was laminar rather than turbulent. In turbulent flow a similar effect was seen but was not significant ($t = 1.2$, $n = 30$). In other words, there may be some slight chromatic differences in the way light is transmitted through flowing water consistent with the fact that light scattering tends to be inversely proportional to a power of wavelength (less scattering at 700 nm than at 470 nm).

The differences between laminar flow and turbulent flow were unmistakable. Turbulence had a strong effect relative to laminar flow, increasing the number of peaks sec-1 ($P < 0.001$ at both 470 and 700 nm). With more peaks in turbulent flow than in laminar flow, their voltage was decreased ($P < 0.001$ at both 470 and 700 nm). In other words, faster peaks did not rise to the same voltage as slower peaks and were shorter in duration (all at $P < 0.001$). The maximum peak voltage reached in turbulent flow was less than in laminar flow ($P < 0.001$). Thus, with lensing in laminar flow on flat steps of an escarpment more light penetrates into the depth of the water for photosynthesis than in the vertical steps where both lensing and shadowing by bubbles reduce the light for photosynthesis.

Table 1: Summary of dynamic measurements with three replicates of the experiment changing photomultiplier connections ($n = 30$)

	Laminar flow		Turbulent flow	
Wavelength	470 nm	700 nm	470 nm	700 nm
Peaks sec $^{-1}$	154 ± 68	128 ± 45	259 ± 12	250 ± 9
Mean peak v	2.3 ± 0.6	2.9 ± 0.7	1.1 ± 0.9	1.4 ± 1.3
Mean peak width sec	0.006 ± 0.002	0.006 ± 0.002	0.003 ± 0.001	0.003 ± 0.0001
Total light	1.82 ± 0.53	2.25 ± 0.59	0.79 ± 0.64	1.05 ± 0.96
Max peak v	7.8 ± 1.8	9.3 ± 1.1	4.92 ± 1.2	6.9 ± 2.2

The personal observation that prompted these experiments was that flat steps with laminar flow on rivers and streams flowing over the Niagara Escarpment tend to have a thick growth of mosses while there appears to be minimal moss growth underneath vertical waterfalls. There are many difficulties in reducing this to a simple explanation involving light penetration for photosynthesis. Turbulence in vertical waterfalls may make it difficult or impossible for mosses to gain anchorage for germination, and in the low run off of summer months there may be a laminar flow of water over waterfalls. This might be a starting point for further ecological studies – just as the possible chromatic differences for total light in laminar flow (Table 1) need to be confirmed by other researchers with different model systems. But this does raise an interesting question in other areas – UV light is widely used as a germicide for water purification. So a follow up experiment was to use the apparatus in Figure 1 with an expanded range in the spectrum.

Filter wheels were rotated to empty positions to allow all light entering the lights guides to reach the photomultipliers, then two different illuminators were used, one with a with a 365 nm fluorescent tube and one with light from the tungsten filament passing through an infrared interference filter at 850 nm.

Table 2. Results with laminar flow and two different illuminators

	365 nm	850 nm
Peaks sec $^{-1}$	122 ± 2	175 ± 6.1
Mean peak v	0.95 ± 0.3	1.25 ± 0.11
Mean peak width sec	0.006 ± 0.0001	0.004 ± 0.0002
Total light	0.75 ± 0.03	0.94 ± 0.08
Max peak v	1.84 ± 0.09	4.96 ± 0.90

Results for light penetration at 850 nm were much higher than for light at 365 nm (all $P < 0.001$ with 2-tails, $n = 10$, in Table 2). The experiment was repeated with a similar result. This agrees with the differences detected for total photosynthetic light in laminar flow (Table 1). Thus, differences in light scattering as a function of wavelength may dominate over absorbance following the Lambert-Beer Law.

Conclusions

For very shallow waters, with depths measured in centimeters rather than meters, the classical analysis of the attenuation of light in deep water is incomplete. In the top centimeter of laminar and turbulent flow, refraction from surface lenses and shadowing by bubbles predominates, so that visible light at long wavelengths has greater penetration than light at shorter wavelengths (700 > 470 nm). This differs from the penetration light into deep water columns following the Lambert-Beer Law.

References

1. Swatland HJ (2017) Colored clays in a groundwater stream, correlating fiber-optic reflectance with electrical impedance. Hydrology Current Research 8: 1-4.
2. Swatland HJ (2012) Groundwater temperature and degassing in the Mad River subwatershed of Lake Huron. Journal of Great Lakes Research 38: 117-120.
3. Hauer FR, Lamberti GA (2007) Methods in Stream Ecology. Elsevier, Amsterdam.
4. NakamuraT, Yamasaki H (2008) Flicker light effects on photosynthetic algae in the reef-building coral Acropora digitifera (Cnidaria: Anthozoa: Scleractinia). Pacific Science 62: 341-350.
5. Iluz D, Alexandrovich I, Dubinsky Z (2012) The enhancement of photosynthesis by fluctuating light. Artificial Photosynthesis 288: 116-133.
6. Allahverdiyeva Y, Suorsa M, Tikkanen M, Aro E-M (2015) Photoprotection of photosystems in fluctuating light intensities. Journal of Experimental Botany 66: 2427-2436.
7. Glimes J (2017) Bryophyte Ecology 1: 1-30. http://digitalcommons.mtu.edu/bryophyte-ecology/
8. Kubásek J, Hájek T, Glimes J (2014) Bryophyte photosynthesis in sunflecks: greater relative induction rate than in tracheophytes. Journal of Bryology 36: 110-117.
9. 9. Wolfe SL (1993) Molecular and Cellular Biology. Wadsworth, Belmont, California 371.
10. Kirk JTO (1977) Attenuation of light in natural waters. Australian Journal of Marine and Freshwater Research 28: 97-508.
11. Brito AC, Newton A, Fernandes TF, Tett P (2013) Measuring light attenuation in shallow coastal systems. Journal of Ecosystem and Ecography 3: 1-4.
12. Taylor TT (1981) Paleobotany. McGraw-Hill, New York.
13. Swatland HJ (1998) Computer Operation for Microscope Photometry. CRC Press, Boca Raton, FL.
14. Swatland HJ (1993) Photomultiplier response in a computer-assisted microscope photometer measured with a multiprogrammer. Journal of Computer-Assisted Microscopy 5: 231-235.
15. Swatland HJ (1991) Analysis of signals from a UV fluorescence probe for connective tissue in beef carcasses. Computers and Electronics in Agriculture 6: 225-234.
16. Kerr PF (1977) Optical Mineralogy. 4th edit. McGraw-Hill, New York 75.
17. Selmke M (2019) Bubble optics. Applied Optics 2019: 1-16.